

Improving the Quality Factor of Microwave Compact Resonators by Optimizing their Geometrical Parameters

K. Geerlings, S. Shankar, E. Edwards, L. Frunzio, R.J. Schoelkopf, M.H. Devoret

Department of Applied Physics, Yale University,

New Haven, Connecticut 06520-8284, USA

Abstract

Applications in quantum information processing and photon detectors are stimulating a race to produce the highest possible quality factor on-chip superconducting microwave resonators. We have tested the surface-dominated loss hypothesis by systematically studying the role of geometrical parameters on the internal quality factors of compact resonators patterned in Nb on sapphire. Their single-photon internal quality factors were found to increase with the distance between capacitor fingers, the width of the capacitor fingers, and the resonator impedance. Quality factors were improved from 210,000 to 500,000 at $T = 200$ mK. All of these results are consistent with our starting hypothesis.

Improving the internal quality factor of on-chip microwave superconducting resonators is a key development for quantum information processing and photon detectors [1, 2]. The internal quality factor at single-photon powers, Q_i , of particular interest for quantum information applications, is observed to be 10-100 times lower than high-power quality factors [3–7]. Ideas for increasing resonator Q_i include switching from conventional metals like Nb or Al to alloys such as TiN or NbTiN [4, 5, 8, 9], using interface layers of SiN [4], etching the substrate between traces [5], depositing metal under special conditions [10], or using low loss substrates [7]. Results from these experiments have generated the hypothesis that resonator Q_i is limited by a surface two level system (TLS) distribution [5, 6, 8, 11].

Motivated by a previous study that showed that the Q_i of coplanar waveguide (CPW) resonators increases with increasing gap [11], we extended the idea of geometrical optimization to compact resonators [3, 6, 9]. Compact resonators, as shown in Figure 1, consist of a meander inductor in parallel to an interdigitated capacitor. Their small size makes them an ideal element for multi-qubit processors. While compact resonators have been shown to have similar Q_i as the more widely used CPW resonators [6], they permit more design choices. Here we show that by changing parameters linked to the surface participation ratio, we have optimized these resonators to achieve an improvement by a factor of 2.4 ± 0.2 . We have thus been able to reach a Q_i of 500,000 at a resonator temperature of 200 mK, our point of reference. In this paper, we prefer to quote Q_i at this temperature because we believe that even when the sample box is anchored to a colder plate, resonator temperatures substantially below 200 mK may not be reached reliably. We return to this point later in the paper.

We measure the quality factor of our compact resonators by performing a microwave transmission experiment. Coupling to the resonators is achieved by placing the resonator in a cutout in the ground plane of a CPW feedline, relying on the mutual inductance between the feedline and the resonator inductor. This coupling introduces a second quality factor, the coupling quality factor Q_c . Typical values of Q_c that we designed ranged from 20,000 to 150,000. As a control experiment, we have designed and measured resonators with Q_c as high as 1.6×10^6 with no change in Q_i . As shown in [10, 12], the measurement of microwave transmission S_{21} through the feedline as a function of frequency ω provides access to Q_i . Although simple resonator models predict a symmetric S_{21} response, the measured response is typically asymmetric due to reflections in the feedline circuit, as shown in Figure 2. Nevertheless, the theory of the arbitrary linear circuit model with one pole and perfect transmission at zero frequency shows that the asymmetric response can

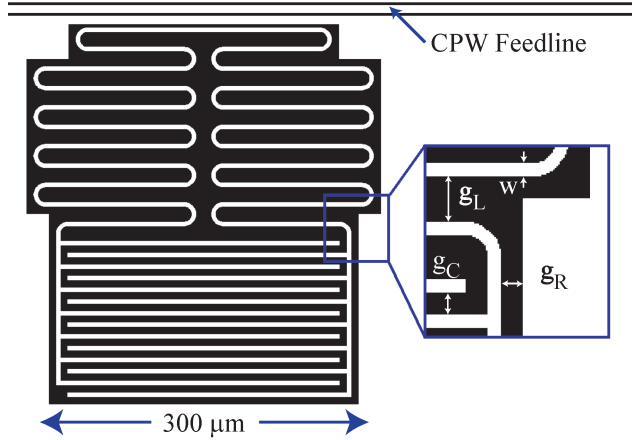


Figure 1: Schematic of compact resonator and inset showing resonator parameters. The compact resonator is coupled inductively to the CPW feedline. The parameters indicated in the inset directly affect the participation of the insulator and metal surfaces to the reactive elements of the resonator.

still be fit to separately extract Q_c and Q_i by introducing an extra parameter $\delta\omega$ characterizing the asymmetry. We thus analyze our data with Equation 1, where the total quality factor, Q_0 , is defined as $1/Q_0 = 1/Q_i + 1/Q_c$.

$$S_{21} = 1 - \frac{\frac{Q_0}{Q_c} - 2iQ_0 \frac{\delta\omega}{\omega_0}}{1 + 2iQ_0 \frac{\omega - \omega_0}{\omega_0}} \quad (1)$$

This expression is exactly equivalent to Eq. (13) in [12] and to Eq. (3) in [10] with a different parametrization.

In our measurement setup, we cool 4 chips at once in a dilution refrigerator with a base temperature of 80 mK (sample temperature of approximately 200 mK). Since each of our chips contained one feedline coupled to 6 independent resonators at frequencies between 5 and 8 GHz, 24 resonators were tested in each cooldown. The chips were wire-bonded to a printed circuit board with Arlon dielectric and placed inside a copper sample box. The box was mounted inside a magnetic shield (Amuneal A4K) and attenuators were installed totaling 50 dB on the input microwave line. All four chips were excited simultaneously using a passive 4-way microwave splitter. The output line consisted of two Pamtech 4-8 GHz isolators on the mixing chamber, a 12 GHz low-pass filter on the 700 mK stage, and a Caltech HEMT amplifier at the 4 K stage. The measurement line was switched between the 4 chips using a microwave switch (Radiall R573423600) mounted on the mixing chamber.

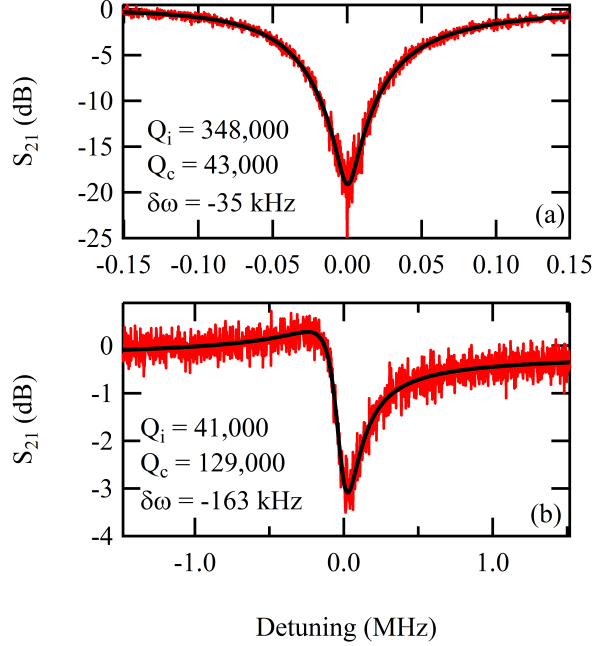


Figure 2: Two extreme examples of resonator response curves fit with Equation 1. Responses typically fall in between (a) symmetric, and (b) strongly asymmetric about the resonant frequency.

Our resonators were fabricated using etched Nb on c-plane sapphire. Before metal deposition, the sapphire surface was prepared by a 60 s ion-milling using a 3 cm Kaufmann source that shoots 500 eV Argon ions at our wafer. Our source operates at a flow rate of 4.25 sccm and a pressure of about $10 \mu\text{Torr}$, generating a current density of 0.67 mA/cm^2 . A 200 nm layer of Nb was then dc magnetron sputtered on the wafer. Photolithography was performed by patterning directly onto S1808 resist using a 365 nm laser. After development, the Nb was etched using a 1:2 mixture of Ar:SF₆ at 10 mTorr for 3 minutes. The wafer was then diced into individual chips for measurement.

In the systematic variation of compact resonator parameters, we chose to optimize the following parameters shown pictorially in Figure 1; the gap g_C between two adjacent capacitor fingers, the distance g_L between two adjacent inductor meanders, the distance g_R between the resonator and the surrounding ground plane, and the width w of the resonator traces. In addition, we also varied the characteristic impedance Z_0 of the resonator. This set of parameters is relevant for surface losses.

We formed a benchmark set of resonators with parameter values: $g_C = 10 \mu\text{m}$, $g_L = 20 \mu\text{m}$, $g_R = 10 \mu\text{m}$, $w = 5 \mu\text{m}$ and $Z_0 = 100 \Omega$. Resonators with this set of parameters will now be called “Design A” resonators. We measured 25 Design A resonators with an average Q_i of $160,000(\pm 20,000)$

g_C (μm)	3	5	10	20	30	40	
ΔQ_i	-31%	-14%	0%	16%	0%	18%	
g_L (μm)	2	5	10	20	40	60	
ΔQ_i	-6%	-10%	1%	0%	2%	2%	
g_R (μm)		5	10	20	50	100	200
ΔQ_i		28%	0%	-2%	-28%	-24%	-36%
w (μm)		3	5	7	10	20	
ΔQ_i		-16%	0%	17%	16%	60%	
Z_0 (Ω)		50	100	150	200	250	300
ΔQ_i		-12%	0%	26%	33%	19%	33%

Design A

Design B

Figure 3: Dependence of Q_i on parameter values. The changes in Q_i for a given mutant value are reported in reference to the average Q_i (160,000) of Design A with positive values representing improvements. The shaded column indicates the Design A value of that parameter; ΔQ_i in this column is zero by definition. The square in each row with a bold border shows the value chosen for Design B. Parameters for Design C cannot easily be shown on this figure as explained in the main text.

and a maximum of 210,000 at single-photon power. Additionally, one chip with 6 resonators inexplicably had quality factors ranging from 40,000 to 70,000, much lower than the rest; we did not include this chip in the benchmark. Q_i typically increased to around 1×10^6 at a “high” power corresponding to an average of 10^8 photons in the resonator. The resonant frequency typically decreased as the temperature passed below 1.3 K, consistent with TLS loss [11]. These results are consistent with the hypothesis that our benchmark Q_i is controlled by surface losses.

We measured 24 geometrical variants of Design A, with each “mutant” resonator having only one parameter value that is changed. For example, the mutant values of g_C were: 3, 5, 20, 30, and 40 μm . The results of the mutant resonators are shown in Figure 3; percent changes in Q_i are given with respect to the Design A resonator benchmark.

For g_C , small values lead to lower Q_i , and larger values lead to higher Q_i . The effect of changing g_L on Q_i is at least a factor of three smaller than for g_C . Thus the gaps where electric fields are present (the capacitor and not the inductor), partially control Q_i , consistent with a surface loss mechanism coupled to the electric field. Similarly Q_i increases for larger w , again consistent with surface loss since wider traces lead to decreasing electric field strength at surfaces. Next, we find that Q_i drops by roughly 25% if $g_R \geq 50 \mu\text{m}$, suggesting that the ground plane prevents electric fields from reaching lossy materials such as the copper box or PCB dielectric. Lastly, the trend

indicating that larger values of Z_0 are beneficial to Q_i appears to contradict the usual hypothesis that dissipative mechanisms have a constant $\tan \delta$. The results for g_C , g_L and w are all consistent with a loss dominated by surface electric field participation.

We chose two new sets of parameters from these results with the goal of improving the Q_i . Resonators with these parameters are called Design B and Design C resonators. Design B values were chosen to be relatively modest changes from Design A, while Design C values were chosen to maximize Q_i . Design B chosen values were: $g_C = 20 \mu\text{m}$, $g_L = 5 \mu\text{m}$, $g_R = 10 \mu\text{m}$, $w = 10 \mu\text{m}$ and $Z_0 = 200 \Omega$. Resonator size increases rapidly with g_L since the larger Z_0 requires twice the inductance. Therefore, to limit the overall size to roughly $700 \mu\text{m} \times 500 \mu\text{m}$, we reduced g_L to $5 \mu\text{m}$, despite the fact that this may lower Q_i by 10%. Design C chosen values were: $g_C = 80 \mu\text{m}$, $g_L = 10 \mu\text{m}$, $g_R = 10 \mu\text{m}$ and $Z_0 = 300 \Omega$. Note that g_C was chosen beyond the range of tested mutant Design A resonators. Also in Design C, the trace width w was different for the capacitor ($40 \mu\text{m}$) and inductor ($10 \mu\text{m}$) halves in order to benefit from the larger capacitor width while keeping the resonator from being larger than $1000 \mu\text{m} \times 1000 \mu\text{m}$.

The results of all 49 Design A, 73 Design B, and 28 Design C resonators are shown in Figure 4. Design B and C each show significantly higher Q_i than Design A, with Design C on average better than Design B. While there exists a spread in Q_i for each design, we observed an overall increase in the range of measured Q_i . The maximum/median Q_i rose from 210,000/160,000 for Design A to 370,000/280,000 for Design B and 500,000/380,000 for Design C.

When ion-milling was not performed, the maximum/median Q_i was reduced to 50,000/30,000 for Design A and 190,000/80,000 for Design B (Design C was not measured without ion-milling). For both Design A and B, the median quality factor was reduced by roughly a factor of four when ion-milling was left out during fabrication. Since this type of cleaning affects only the substrate-air interface and substrate-metal interface, we infer that these two surfaces participate strongly. The dominating participation of these surfaces has also been predicted by simulation [13]. This Q_i dependence on ion-milling also suggests that while the geometry controls the resonator sensitivity to the surface loss mechanism, the surface preparation determines the strength of the loss.

When re-measured in a dilution refrigerator with a lower base temperature (15mK), we found that resonator Q_i drops by roughly a factor of 2, which is consistent with TLS loss [11]. We have measured similar resonators coupled to a qubit and found that their temperatures would not reach below 50 mK, as also reported by other groups [14]. However, directly measuring the linear resonator temperature without a qubit to add nonlinearity is outside the scope of this study. Reas-

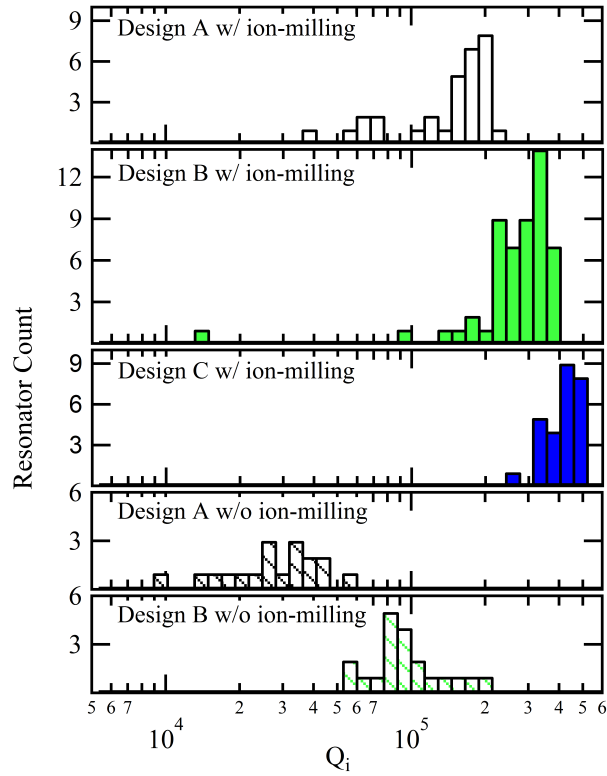


Figure 4: Histograms of single-photon internal quality factors for designs A, B, and C resonators with ion-milling and designs A and B without ion-milling. For both Design A and Design B resonators, when ion-milling is not performed, Q_i is roughly a factor of four lower.

surprisingly, the increase of Q_i from Design A to B to C resonators remains even at lower temperatures; indicating that the geometric variation affects only the sensitivity to loss, not the absolute strength.

In conclusion, we have shown that the Q_i of compact resonators depends strongly on geometrical factors controlling where electric fields are stored. In addition, substrate surface preparation prior to metal deposition is crucial. Using our results indicating that surface loss is dominant, we have been able to increase, at our point of reference temperature of 200 mK, the maximum internal quality factor of our resonators from 210,000 to 500,000.

The authors thank Danielle Braje at MIT-LL for an independent measurement of our resonators. This research was supported by IARPA under grant W911NF-09-1-0369 and ARO under grant

- [1] H. Wang, M. Mariantoni, R. C. Bialczak, M. Lenander, E. Lucero, M. Neeley, A. D. O'Connell, D. Sank, M. Weides, J. Wenner, et al., *Phys. Rev. Lett.* **106**, 060401 (2011).
- [2] B. A. Mazin, B. Bumble, P. K. Day, M. E. Eckart, S. Golwala, J. Zmuidzinas, and F. A. Harrison, *Appl. Phys. Lett.* **89**, 222507 (2006).
- [3] T. Lindstroem, J. E. Healey, M. S. Colclough, C. M. Muirhead, and A. Y. Tzalenchuk, *Phys. Rev. B* **80**, 132501 (2009).
- [4] M. R. Vissers, J. Gao, D. S. Wisbey, D. A. Hite, C. C. Tsuei, A. D. Corcoles, M. Steffen, and D. P. Pappas, *Appl. Phys. Lett.* **97**, 232509 (2010).
- [5] R. Barends, N. Vercruyssen, A. Endo, P. J. de Visser, T. Zijlstra, T. M. Klapwijk, P. Diener, S. J. C. Yates, and J. J. A. Baselmans, *Appl. Phys. Lett.* **97**, 023508 (2010).
- [6] M. Khalil, F. Wellstood, and K. Osborn, *Applied Superconductivity, IEEE Transactions on* **21**, 879 (2011).
- [7] S. J. Weber, K. W. Murch, D. H. Slichter, R. Vijay, and I. Siddiqi, *Appl. Phys. Lett.* **98**, 172510 (2011).
- [8] R. Barends, H. L. Hortensius, T. Zijlstra, J. J. A. Baselmans, S. J. C. Yates, J. R. Gao, and T. M. Klapwijk, *Appl. Phys. Lett.* **92**, 223502 (2008).
- [9] H. G. Leduc, B. Bumble, P. K. Day, B. H. Eom, J. Gao, S. Golwala, B. A. Mazin, S. McHugh, A. Merrill, D. C. Moore, et al., *Appl. Phys. Lett.* **97**, 102509 (2010).
- [10] A. Megrant, C. Neill, R. Barends, B. Chiaro, Y. Chen, L. Feigl, J. Kelly, E. Lucero, M. Mariantoni, P. J. J. O'Malley, et al., *Appl. Phys. Lett.* **100**, 113510 (2012).
- [11] J. S. Gao, M. Daal, A. Vayonakis, S. Kumar, J. Zmuidzinas, B. Sadoulet, B. A. Mazin, P. K. Day, and H. G. Leduc, *Appl. Phys. Lett.* **92**, 152505 (2008).
- [12] M. S. Khalil, M. J. A. Stoutimore, F. C. Wellstood, and K. D. Osborn, *J. Appl. Phys.* **111**, 054510 (2012).
- [13] J. Wenner, R. Barends, R. C. Bialczak, Y. Chen, J. Kelly, E. Lucero, M. Mariantoni, A. Megrant, P. J. J. O'Malley, D. Sank, et al., *Appl. Phys. Lett.* **99**, 113513 (2011).
- [14] A. D. Corcoles, J. M. Chow, J. M. Gambetta, C. Rigetti, J. R. Rozen, G. A. Keefe, M. B. Rothwell, M. B. Ketchen, and M. Steffen, *Appl. Phys. Lett.* **99**, 181906 (2011).